ChemComm

ROYAL SOCIETY OF CHEMISTRY

COMMUNICATION

View Article Online
View Journal | View Issue

Cite this: *Chem. Commun.*, 2021, **57**, 2780

Received 3rd December 2020,
Accepted 8th February 2021

DOI: 10.1039/d0cc07886g

rsc.li/chemcomm

A proton-responsive ligand becomes a dimetal linker for multisubstrate assembly *via* nitrate deoxygenation†

Alyssa C. Cabelof, Veronica Carta and Kenneth G. Caulton *

A bidentate pyrazolylpyridine ligand (HL) was installed on divalent nickel to give $[(HL)_2Ni(NO_3)]NO_3$. This compound reacts with a bis-silylated heterocycle, 1,4-bis-(trimethylsilyl)-1,4-diaza-2,5-cyclohexadiene (TMS_2Pz) to simultaneously reduce one of the nitrate ligands and deprotonate one of the HL ligands, giving octahedral $(HL)(L^-)Ni(NO_3)$. The mononitrate species formed is then further reacted with TMS_2Pz to doubly deoxygenate nitrate and form $[(L^-)Ni(NO)]_2$, dimeric *via* bridging pyrazolate with bent nitrosyl ligands, representing a two-electron reduction of coordinated nitrate. Independent synthesis of a dimeric species $[(L^-)Ni(Br)]_2$ is reported and effectively assembles two metals with better atom economy.

Carbon dioxide reduction is a primary focus of current catalytic interest because the accumulation of carbon dioxide in the planetary atmosphere causes global warming due to the greenhouse effect.[1] The widespread use of ammonia fertilizers contributes to nitrate runoff from farm fields, which creates "dead zones" in lakes, bays and coastal regions.[2] Thus, similar to high oxidation state carbon, high oxidation state nitrogen becomes another target of chemical deoxygenation approaches for remediation purposes, with the goal to recycle the nitrogen into value added compounds. Nitrate reduction has been accomplished by photochemical[3] and electrochemical[2a,4] means, along with the use of chemical reductants or *via* deoxygenation.[5] Bis-silyl dihydropyrazines[6] have been shown to be effective for deoxygenations of organic NO_x compounds[7] and metal-mediated nitrate deoxygenations for complexes carrying multiple nitrate or nitrite ligands.[5f,g,8]

This work builds on these existing reductive deoxygenations by using a proton responsive pyrazolylpyridine ligand that provides redox flexibility whether it is neutral or deprotonated. The pyrazolylpyridine ligand has been used primarily as a source of a monoanionic bidentate ligand to replace phenylpyridyl as an optical tuning component in luminescent metal complexes.[9] It has also attracted interest for applications in magnetism[10] and crystal engineering.[11] We envisioned that in the deprotonated state, the pyrazolate moiety will have the ability to bridge multiple metal centers,[11a,12] allowing for the formation of bimetallic species with two nitrogen oxyanions in close proximity. This might allow, under reducing conditions, the formation of N–N bonds from nitrate. In this case, NN bond formation is an intramolecular process, hence with minimal entropy loss. Current efforts focus on this intramolecular process.[12d,13]

We initially targeted two bidentate ligands *per* Ni, and therefore reacted 2-methyl-6-[5(3)-phenyl-1*H*-pyrazol-3(5)-yl]-pyridine (HL) with $Ni(NO_3)_2{\cdot}6H_2O$ at a 2 : 1 mole ratio in DCM (Scheme 1a). 4 hours of stirring afforded a light blue material which was characterized by ^1H NMR spectroscopy and shown to be paramagnetic, implying either tetrahedral or octahedral Ni(II). Single crystal X-ray diffraction studies establish a

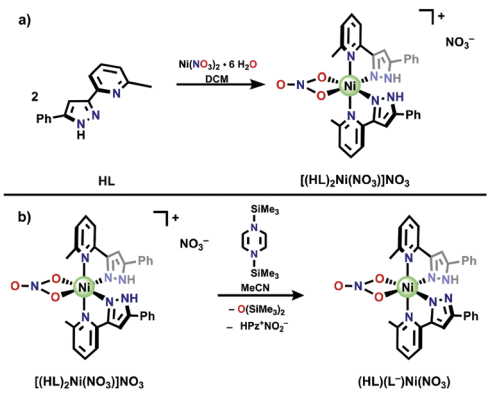

Scheme 1 (a) Synthesis of $[(HL)_2Ni(NO_3)]NO_3$ and (b) its conversion to $(HL)(L^-)Ni(NO_3)$ *via* deoxygenation and subsequent deprotonation with TMS_2Pz.

Department of Chemistry, Indiana University, 800 E. Kirkwood Ave., Bloomington, IN, 47401, USA. E-mail: caulton@indiana.edu

† Electronic supplementary information (ESI) available: NMR, FT-IR, and crystal structure data for $[(HL)_2Ni(NO_3)]NO_3$ (CCDC: 2042062), $(HL)(L^-)Ni(NO_3)$ (CCDC: 2042063), $[(L^-)Ni(NO)]_2$ (CCDC: 2042064), $[(HL)NiBr_2]_2$ (CCDC: 2044737), $(HL)NiBr_2$ (CCDC: 2044738) and $[(L^-)Ni(Br)(MeCN)]_2$ (CCDC: 2042065). For ESI and crystallographic data in CIF or other electronic format see DOI: 10.1039/d0cc07886g

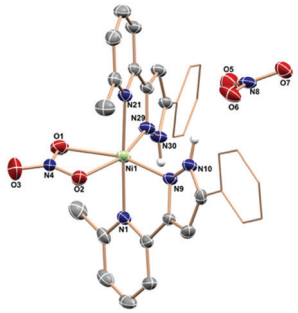

Fig. 1 Molecular structure (50% probability ellipsoids) of $[(HL)_2Ni(NO_3)]NO_3$ showing selected atom labelling; unlabelled atoms are carbon. All protons except pyrazole NH protons have been removed for clarity. Ni1–O2, 2.1364(16) Å; Ni1–O1, 2.1545(17); Ni1–N21, 2.1473(17); Ni1–N29, 2.0176(18); Ni1–N9, 2.0197(18); Ni1–N1, 2.1260(18).

compound with the formula $[(HL)_2Ni(NO_3)]NO_3$, where one nitrate is coordinated bidentate to Ni and the other is a counterion that interacts strongly with the ligand through hydrogen bonding to pyrazole (Fig. 1). We sought deoxygenation initially of one nitrate in $[(HL)_2Ni(NO_3)]NO_3$, and attempted this with the bis-silylated heterocycle, 1,4-bis-(trimethylsilyl)-1,4-diaza-2,5-cyclohexadiene (TMS_2Pz). Reaction of $[(HL)_2Ni(NO_3)]NO_3$ with TMS_2Pz at a 1 : 1 mole ratio in MeCN (Scheme 1b) occurs with a color change from light blue to teal within 30 minutes. After 12 h of stirring with no further color changes, volatiles were removed and a teal paramagnetic species was isolated. Single crystal X-ray diffraction of crystals grown by diffusion of pentane vapors into a concentrated THF solution revealed a formula $(HL)(L^-)Ni(NO_3)$ (Fig. 2a). One of the bidentate ligands has a pyrazole with an N–N–C angle $< 108.5^\circ$ (indicating a lone pair on N)[14] while the other has an angle $>111.3^\circ$ (consistent with H on the N). Ligand deprotonation at only one site is supported by two molecules in the asymmetric unit forming a hydrogen bonded dimer between the protonated pyrazole and the deprotonated pyrazolate (Fig. 2b). The octahedral nickel atoms both show one large N–Ni–N angle involving pyrazole and pyrazolate, $>111.0^\circ$, and this opens each $(HL)(L^-)Ni(NO_3)$ unit for this hydrogen bonded dimerization.

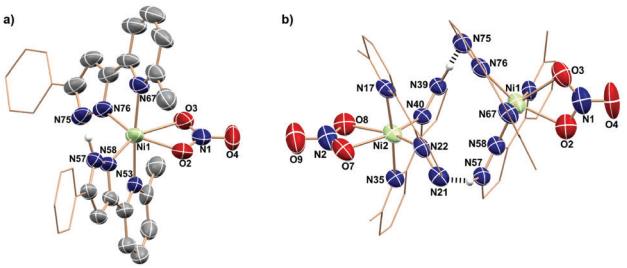

Fig. 2 (a) Molecular structure (50% probability ellipsoids) of one molecule of $(HL)(L^-)Ni(NO_3)$, showing selected atom labelling; only the NH proton is shown (on N57). Selected structural parameters: Ni1–O2, 2.115(6) Å; Ni1–O3, 2.211(6); Ni1–N53, 2.143(7); Ni1–N58, 2.060(7); Ni1–N67, 2.125(8); Ni1–N76, 2.000(8); O2–N1, 1.270(10); O3–N1, 1.296(10); O4–N1, 1.210(9); values for the second crystallographically independent Ni show no notable deviations from these and (b) view of the $[(HL)(L^-)Ni(NO_3)]_2$ dimer. Hydrogen bonds are shown with dashed lines. Phenyl groups are shown as wireframe.

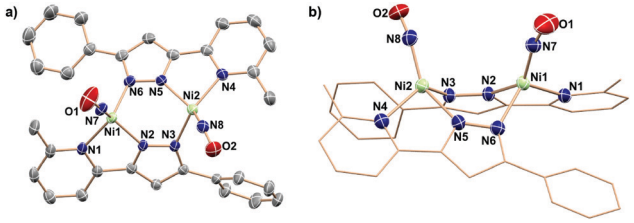

Fig. 3 Molecular structure (50% probability ellipsoids) of $[(L^-)Ni(NO)]_2$ showing (a) top view of the non-hydrogen atoms and (b) side-on view with selected structural parameters: Ni1–N2, 1.9840(16); Ni1–N1, 2.0737(18); Ni1–N6, 2.0040(17); Ni1–N7, 1.6470(19); N7–O1, 1.164(3); O1–N7–Ni1, 165.72(19).

Following this reaction progress by ^1H NMR spectroscopy shows the unambiguous formation of hexamethyldisiloxane, indicating that a deoxygenation event occurred. Therefore, we propose that deoxygenation of one of the nitrate ligands in $[(HL)_2Ni(NO_3)]NO_3$ gives $(HL)_2Ni(NO_3)(NO_2)$ as an intermediate, and the emerging pyrazine byproduct acts as a base[8] to deprotonate one of the neutral HL ligands and departs with the deoxygenated nitrite to give the crystallographically characterized product, $(HL)(L^-)Ni(NO_3)$. Our attempts to observe or trap the mixed nitrate/nitrite intermediate were unsuccessful; no intermediate nickel complex signals are observed on the NMR timescale. The simultaneous deoxygenation of nitrate and deprotonation of one HL ligand forms a molecular mononitrate species.

We attempted further deoxygenation of $(HL)(L^-)Ni(NO_3)$ with two equivalents of TMS_2Pz, targeting $(HL)(L^-)Ni(NO)$. This reaction proceeds rapidly in THF with a color change from teal to dark green within 5 minutes. Following the reaction progress by ^1H NMR spectroscopy (Fig. S8, ESI†) we observed conversion to a diamagnetic species and the expected two stoichiometric equivalents of hexamethyldisiloxane and pyrazine. The infrared spectrum confirms the absence of –NH and contains a band at 1729 cm^{-1}, consistent with a nitrosyl ligand. Single crystal X-ray diffraction studies establish a dimeric compound with the formula $[(L^-)Ni(NO)]_2$ (Fig. 3). Geometry about each Ni center is best described as seesaw (τ_4 values[15] = 0.41 and 0.35 for Ni1 and Ni2 respectively) and is held into a dimer by bridging pyrazolate. The two nitrosyl ligands are bent slightly, with Ni1–N7–O1 angle of 165.7° and Ni2–N8–O2 angle of 148.4°. Although the nitrosyl angles are slightly bent which might suggest NO• or even NO^-, the diamagnetism of this compound suggests that the nickel centers are best described as Ni^0 and thus, the nitrosyls are NO^+. This transformation is accompanied by the loss of a neutral HL ligand, which is confirmed by ^1H NMR spectroscopy, after washing

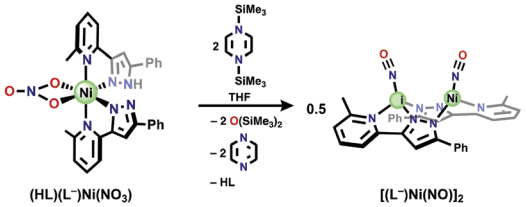

Scheme 2 Balanced reaction for formation of $[(L^-)Ni(NO)]_2$.

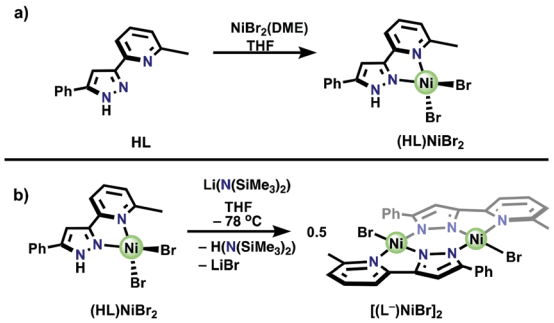

Scheme 3 (a) Synthesis of $(HL)NiBr_2$ and (b) dehydrohalogenation of $(HL)NiBr_2$ to form $[(L^-)NiBr]_2$.

the crude material with diethyl ether to collect HL. The overall balanced reaction for this transformation is shown in Scheme 2. We propose that ligand loss occurs when the nitrosyl is formed, which exerts a strong trans effect and liberates neutral HL, then dimerization gives the stable 18 valence electron species $[(L^-)Ni(NO)]_2$. The pendent pyridyl donor in this ligand has the flexibility to form a seesaw structure with Ni, and is not limited to planar and octahedral metal preferences.

Due to the loss of half of the ligand from the original $[(HL)_2Ni(NO_3)]NO_3$, we sought a route to a bimetallic species with better atom economy. Our first attempts at this simply altered the stoichiometry shown in Scheme 1a from a 2 : 1 ligand : metal ratio to a 1 : 1, but regardless of the equivalents of ligand delivered, $[(HL)_2Ni(NO_3)]NO_3$ preferentially forms. We attribute this to the very poor solubility of the nickel source, $Ni(NO_3)_2{\cdot}6H_2O$, causing a high concentration of ligand in solution compared to metal reagent. We therefore turned to reaction of HL with a more soluble metal starting material, $NiBr_2(DME)$ (DME = dimethoxyethane) according to Scheme 3a. This reaction proceeds in THF solution to give a single, paramagnetic complex, with evidence of only one ligand per metal by mass spectrometry. The product is orange in the solid state, but upon dissolution in THF solvent, a notable color change to bright pink is observed (Fig. S1, ESI†). This color change is reversible. Crystals were grown by vapor diffusion of either pentane or diethyl ether vapors into a concentrated THF solution, and two different crystalline materials are present with detectably different colors. The majority of the crystalline material is orange (<95%) with a small amount of pink crystals (>5%) present. Single crystal XRD establishes the chemical formula of the orange crystals as $[(HL)NiBr_2]_2$, dimeric by bromide bridging (Fig. 4a). This structure might suggest that HL is insufficiently bulky for the metal to achieve coordination number four. However, single crystal XRD of the pink crystals shows that a four-coordinate tetrahedral (τ_4 = 0.84) monomer with formula $(HL)NiBr_2$ is formed, with no bromide bridges and with a THF molecule hydrogen bonding to the pyrazole NH (Fig. 4b). It is especially interesting that the presence of THF in the solid state does not lead to five coordinate nickel *via* THF coordination. Since monomer and dimer form concurrently the energy difference between the two must be small. Overall, this should have no significant influence on chemical reactivity, but it represents an opportunity to compare monomer and dimer structures (see ESI†).

This new species was then reacted with lithium bis-(trimethylsilyl)amide (LiHMDS) in THF at −78 °C (Scheme 3b), where a color change from orange to light green was observed in the time of mixing. The product was characterized as a single paramagnetic species, distinct from starting material. Single crystals were grown by slow evaporation of acetonitrile, establishing the formula of this compound as $[(L^-)Ni(Br)(MeCN)]_2$ (Fig. 4c), and confirming that this dehydrohalogenation route successfully generates a dimeric species without sacrificing a ligand; coordination of acetonitrile is due to crystal growth conditions. The dimer is centrosymmetric with two 5-coordinate nickel centers and is best described as a distorted square pyramid (τ_4 value = 0.16). The Ni1-Ni2 distance is 3.821 Å and is therefore non-bonding.

This work highlights the potency of TMS_2Pz for deoxygenations of coordinated nitrate anions along with showing the possibility of deprotonation *via* emerging pyrazine base as an unintended side reaction of deoxygenation. All together, this work details the cooperative efforts of a proton responsive ligand and TMS_2Pz in formation of the bimetallic species $[(L^-)Ni(NO)]_2$. Dehydrohalogenation of $(HL)NiBr_2$ is an effective way this pyrazolylpyridine ligand naturally accomplishes

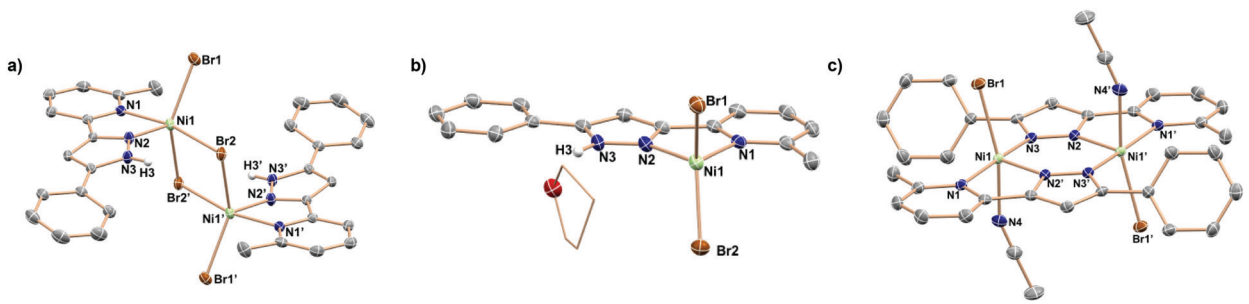

Fig. 4 Molecular structure (50% probability ellipsoids) showing selected structural parameters of (a) $[(HL)NiBr_2]_2$: Br2–Ni1, 2.4849(3); Br2–Ni1′, 2.5506(3); Br1–Ni1, 2.4235(3); Ni1–N1, 2.1005(15); Ni1–N2, 1.9834(15); Br1–Ni1–Br2, 140.284(11); N1–Ni1–Br2′,167.61(4), (b) $(HL)NiBr_2$: Br1–Ni1, 2.3527(4); Br2–Ni1, 2.3552(4); Ni1–N1, 2.019(2); Ni1–N2, 1.983(2); Br1–Ni1–Br2, 129.928(17); N1–Ni1–Br1, 111.51(6); N1–Ni1–Br2, 106.35(6); N2–Ni1–Br1, 108.79(7); N2–Ni1–Br2, 108.24(6), (c) $[(L^-)Ni(Br)(MeCN)]_2$: Br1–Ni1, 2.4888(3); Ni1–N2, 1.9851(17); Ni1–N3′, 2.0067(18); Ni1–N1, 2.0800(18); Ni1–N4, 2.0997(19); N4–Ni1–Br1, 164.16(6); N3′–Ni1–N1, 173.71.

assembly of two metal centers to form $[(L^{-})NiBr]_2$, which will offer routes to $[(L^{-})Ni(NO)]_2$ with better ligand atom economy. This dimeric species also provides the potential for installing two nitrogen oxyanion substrates for subsequent reductive deoxygenation.

This work was supported by the Indiana University Office of Vice President for Research and the National Science Foundation by grant CHE-1362127. Support for the acquisition of the Bruker Venture D8 diffractometer through the Major Scientific Research Equipment Fund from the President of Indiana University is gratefully acknowledged.

Conflicts of interest

There are no conflicts of interest to declare.

Notes and references

1 (*a*) A. J. Morris, G. J. Meyer and E. Fujita, *Acc. Chem. Res.*, 2009, **42**, 1983; (*b*) J. Qiao, Y. Liu, F. Hong and J. Zhang, *Chem. Soc. Rev.*, 2014, **43**, 631; (*c*) S. Drouet, M. Robert, C. Costentin and J.-M. Savéant, *Science*, 2012, **338**, 90; (*d*) B. Schille, M. Roemelt and R. Francke, *Chem. Rev.*, 2018, **118**, 4631; (*e*) Y. Y. Birdja, E. Pérez-Gallent, M. C. Figueiredo, A. J. Göttle, F. Calle-Vallejo and M. T. M. Koper, *Nat. Energy*, 2019, **4**, 732; (*f*) S. Nitopi, E. Bertheussen, S. B. Scott, X. Liu, A. K. Engstfeld, S. Horch, B. Seger, I. E. L. Stephens, K. Chan, C. Hahn, J. K. Nørskov, T. F. Jaramillo and I. Chorkendorff, *Chem. Rev.*, 2019, **119**, 7610.

2 (*a*) M. Duca and M. T. M. Koper, *Energy Environ. Sci.*, 2012, **5**, 9726; (*b*) R. Rosenberg and R. J. Diaz, *Science*, 2008, **321**, 926; (*c*) W. W. Bouska, J. L. Eitzmann, T. J. Pilger, K. L. Pitts, A. J. Riley, J. T. Schloesser, D. J. Thornbrugh and W. K. Dodds, *Environ. Sci. Technol.*, 2009, **43**, 12; (*d*) M. A. Sutton, J. Galloway, Z. Klimont, W. Winiwarter and J. W. Erisman, *Nat. Geosci.*, 2008, **1**, 636; (*e*) J. N. Galloway, J. D. Aber, J. W. Erisman, S. P. Seitzinger, R. W. Howarth, E. B. Cowling and B. J. Cosby, *BioScience*, 2003, **53**, 341.

3 (*a*) J. Sá, C. A. Agüera, S. Gross and J. A. Anderson, *Appl. Catal., B*, 2009, **85**, 192; (*b*) M. Shand and J. A. Anderson, *Catal. Sci. Technol.*, 2013, **3**, 879; (*c*) T. Yang, K. Hristovski, P. Westerhoff and K. Doudrick, *Appl. Catal., B*, 2013, **136**, 40.

4 (*a*) J. Shen, Y. Y. Birdja and M. T. M. Koper, *Langmuir*, 2015, **31**, 8495; (*b*) M. Lanzarini-Lopes, K. Hristovski, P. Westerhoff and S. Garcia-Segura, *Appl. Catal., B*, 2018, **236**, 546; (*c*) S. Xu, D. C. Ashley, H.-Y. Kwon, G. R. Ware, C.-H. Chen, Y. Losovyj, X. Gao, E. Jakubikova and J. M. Smith, *Chem. Sci.*, 2018, **9**, 4950; (*d*) J.-X. Liu, D. Richards, N. Singh and B. R. Goldsmith, *ACS Catal.*, 2019, **9**, 7052.

5 (*a*) J. C. Fanning, *Coord. Chem. Rev.*, 2000, **199**, 159; (*b*) C. L. Ford, Y. J. Park, E. M. Matson, Z. Gordon and A. R. Fout, *Science*, 2016, **354**, 741; (*c*) P. L. Damon, G. Wu, N. Kaltsoyannis and T. W. Hayton, *J. Am. Chem. Soc.*, 2016, **138**, 12743; (*d*) M. Delgado and J. D. Gilbertson, *Chem. Commun.*, 2017, **53**, 11249; (*e*) J. Gwak, S. Ahn, M.-H. Baik and Y. Lee, *Chem. Sci.*, 2019, **10**, 4767; (*f*) J. Seo, A. C. Cabelof, C.-H. Chen and K. G. Caulton, *Chem. Sci.*, 2019, **10**, 475; (*g*) D. M. Beagan, V. Carta and K. G. Caulton, *Dalton Trans.*, 2020, **49**, 1681.

6 (*a*) H. Tsurugi, H. Tanahashi, H. Nishiyama, W. Fegler, T. Saito, A. Sauer, J. Okuda and K. Mashima, *J. Am. Chem. Soc.*, 2013, **135**, 5986; (*b*) T. Saito, H. Nishiyama, H. Tanahashi, K. Kawakita, H. Tsurugi and K. Mashima, *J. Am. Chem. Soc.*, 2014, **136**, 5161; (*c*) H. Tsurugi and K. Mashima, *Acc. Chem. Res.*, 2019, **52**, 769.

7 (*a*) A. Bhattacharjee, H. Hosoya, H. Ikeda, K. Nishi, H. Tsurugi and K. Mashima, *Chem. – Eur. J.*, 2018, **24**, 11278; (*b*) D. M. Beagan, I. J. Huerfano, A. V. Polezhaev and K. G. Caulton, *Chem. – Eur. J.*, 2019, **25**, 8105.

8 A. C. Cabelof, V. Carta, C.-H. Chen and K. G. Caulton, *Dalton Trans.*, 2020, **49**, 7891.

9 (*a*) D. Ma, L. Duan, Y. Wei, L. He, L. Wang and Y. Qiu, *Chem. Commun.*, 2014, **50**, 530; (*b*) D. Sykes, S. C. Parker, I. V. Sazanovich, A. Stephenson, J. A. Weinstein and M. D. Ward, *Inorg. Chem.*, 2013, **52**, 10500; (*c*) Y. Liu, P. Zhang, X. Fang, G. Wu, S. Chen, Z. Zhang, H. Chao, W. Tan and L. Xu, *Dalton Trans.*, 2017, **46**, 4777.

10 (*a*) B. A. Leita, B. Moubaraki, K. S. Murray, J. P. Smith and J. D. Cashion, *Chem. Commun.*, 2004, 156; (*b*) B. A. Leita, B. Moubaraki, K. S. Murray and J. P. Smith, *Polyhedron*, 2005, **24**, 2165–2172; (*c*) S.-L. Zhang, X.-H. Zhao, Y.-M. Wang, D. Shao and X.-Y. Wang, *Dalton Trans.*, 2015, **44**, 9682.

11 (*a*) L. F. Jones, K. D. Camm, C. A. Kilner and M. A. Halcrow, *CrystEngComm*, 2006, **8**, 719; (*b*) J. Pons, A. Chadghan, J. Casabó, A. Alvarez-Larena, J. F. Piniella, X. Solans, M. Font-Bardia and J. Ros, *Polyhedron*, 2001, **20**, 1029.

12 (*a*) P. J. Zinn, D. R. Powell, V. W. Day, M. P. Hendrich, T. N. Sorrell and A. S. Borovik, *Inorg. Chem.*, 2006, **45**, 3484; (*b*) A. Prokofieva, A. I. Prikhod'ko, E. A. Enyedy, E. Farkas, W. Maringgele, S. Demeshko, S. Dechert and F. Meyer, *Inorg. Chem.*, 2007, **46**, 4298; (*c*) V. Colombo, S. Galli, H. J. Choi, G. D. Han, A. Maspero, G. Palmisano, N. Masciocchi and J. R. Long, *Chem. Sci.*, 2011, **2**, 1311; (*d*) Y. Arikawa, T. Asayama, Y. Moriguchi, S. Agari and M. Onishi, *J. Am. Chem. Soc.*, 2007, **129**, 14160.

13 E. Ferretti, S. Dechert, S. Demeshko, M. C. Holthausen and F. Meyer, *Angew. Chem., Int. Ed.*, 2019, **58**, 1705.

14 S. Kuwata and T. Ikariya, *Chem. – Eur. J.*, 2011, **17**, 3542.

15 $\tau_4 = (360 - \beta - \alpha)/141$, refer to: L. Yang, D. R. Powell and R. P. Houser, *Dalton Trans.*, 2007, 955.